[1]Chenqi Xie*
[2]Shangwen Wang
[3]Yunlai Yu
[4]Yubo Deng

An Assessment of Geological Hazard Management using Dynamically Stabilized Recurrent Neural Network and Beluga Whale Optimization Algorithm

Abstract: - Mountainous region geological hazards are a leading cause of natural disasters, resulting in significant human and economic losses. Regional topography, landforms, lithology, plant life, geological circumstances, and meteorology all have a significant impact on their creation. Gansu, situated in the interior of Northwestern China, features Lanzhou as its capital and primary urban center, positioned in the southeast of the province. Geological risks, particularly landslides, mudslides, and avalanches, present significant challenges to Gansu Province. Consequently, local authorities are actively devising customized strategies to mitigate these hazards and foster sustainable development. In this research work, an Assessment of Geological Hazard Management using Dynamically Stabilized Recurrent Neural Network and Beluga Whale Optimization Algorithm (AGL-HM-DSRNN-BWOA) is proposed. Initially, the input raster data are gathered from the Normalised Difference Vegetation Index (NDVI) dataset. The input raster data is then pre-processed using Adaptive Actor-Critic Bilateral Filter (A2CBF) to reduce noises and increase the overall quality of the raster data. To classify the geological hazards, the pre-processed raster data are fed into a neural network named DSRNN. The geological hazard is accurately categorized as low risk, medium-low risk, medium-high risk, high risk using proposed DSRNN. In general, DSRNN does not express some adaption of optimization strategies for determining optimal parameters to promise exact classification for managing geological hazard by assessment. Therefore, Beluga Whale Optimization Algorithm (BWOA) is proposed to enhance weight parameter of DSRNN classifier, which precisely assess for managing the geological hazards. The efficiency of the proposed AGL-HM-DSRNN-BWOA approach is evaluated using a number of performance criteria, including accuracy, sensitivity, specificity, ROC, mean square error, root mean square error, mean absolute error. The proposed AGL-HM-DSRNN-BWOA method attains 22.36%, 25.42% and 18.17% higher accuracy, 21.26%, 15.42% and 19.27% higher sensitivity, 28.36%, 25.32% and 28.27% higher F-measure compared with existing methods, such as the Risk assessment and its influencing factors examination of geological hazards in typical mountain environment (RA-IFA-GH-TME), Feasibility study of land cover categorization under normalized difference vegetation index for landslide risk assessment(LCC-NDVI-LRA), and Multiple hazard exposure mapping under machine learning for Salzburg, Austria (MH-EM-SSA-ML) respectively.

Keywords: Adaptive Actor-Critic Bilateral Filter, Beluga Whale Optimization Algorithm, Dynamically Stabilized Recurrent Neural Network, Geological Hazard Management Assessment.

I. INTRODUCTION

Rocky geological risk factors are a leading cause of natural disasters, resulting in significant losses of human and economic. Regional topography, landforms, lithology, vegetation, environmental situations, meteorology all have a significant impact on their creation. Based on topography and structural characteristics, the risk estimation of geological hazards examines the occurrence including regional disasters distribution [1, 2]. Since the twenty-first century, as a fundamental step in forecasting geological risks, developing strategies for disaster prevention and mitigation. Geological hazard risk assessment has gained popularity as a topic among academics and is now a key part of global efforts to prevent and reduce disasters, also play a vital role in disaster management [3, 4]. Gansu Province in China blends history, adventure, and natural wonders, featuring the Gobi Desert and Qilian Mountains alongside ancient Silk Road villages. Iconic Buddhist cave temples such as Mogao Caves and Yungang Grottoes adorn its landscape, adding to its allure. [5, 6]. Several geological hazards, including landslides, debris flows, collapses, and like are common in the area due to its unique environment, which includes manifold rainstorms, highest mountains, more faults. These hazards have become a major barrier to the region's ability to sustain socioeconomic development [7, 8]. Geological hazards like landslides, debris flows, and collapses present a significant obstacle to sustainable socio-economic growth in Gansu Province. There's a pressing need to comprehensively analyze the spatial and temporal dynamics of these hazards [9, 10]. However, research on risk assessment with the factors influencing mountainous geological risks in Gansu remains limited. Given the province's cultural richness, diverse population, and unique traditions, conducting such assessments is crucial amid its rapid expansion and efforts toward balanced, sustainable development [11, 12]. Recent advancements in geographic information system (GIS) led to successful studies on assessing environmental hazards. The investigation of key and influencing factors is not given the same weight as spatial pattern analysis in the present hazards risk estimation [13, 14].

[1,2,3,4*]*The First Geological and Mineral Exploration Institute of Gansu Provincial Geology and Mineral Bureau, Tianshui, Gansu, 741020, China*
[1*]*Corresponding author Email: 13830885488@163.com*

The risk estimation has consistently progressed from qualitative to quantitative analysis from the viewpoint of investigation methodologies. Common assessment models, include analytical hierarchy process (AHP), expert score; fuzzy comprehensive estimation, artificial neural network (ANN), principal component analysis, information quantity mode [15]. The first three quantitative assessment methods have basic operating and implementation requirements. Human subjectivity heavily influences the assignment of index weights during system building. ANN predicts accurately, but the process of modeling is involved; modeling requires more reliable basic data, this is hard to gather large-scale research [16, 17]. The principal component analysis method reduces co-linearity among evaluation indicators by aggregating multiple components into a comprehensive indicator. However, it does not consider the geographical features of the indicators. The mentioned evaluation methodologies have constraints and may not entirely capture the geographical distribution of geological hazards and influencing factors in Gansu. Notably, Gansu is renowned for its water-pipe tobacco cultivation, particularly around Lanzhou and farther west. Moreover, the vast grasslands of Gansu sustain substantial livestock populations, with sheep constituting approximately half of these herds. Nevertheless, the information quantity mode determines the optimal consolidation of important components with bigger contributions for geological hazards, so produce an effectual risk appraisal for hilly geological dangers [18, 19].

Geological hazard is a concept created through the United Nations in the framework of the UN Sustainable Development Goals, as well as Agenda twenty one, which promotes mitigation of risks and disaster preparedness as part of a sustainable development program. Geological-hazard evaluations have risen in recent years, particularly when many natural hazards have afflicted a region. More damage can be done by geological hazards than by any one hazard, as they can jeopardize human life and have an impact on infrastructure, transportation, and the environment. Flooding is a greatest risks posed by nature that has occurred on a regular basis in recent years around the world. These drawbacks in the existing approaches motivated to do this work.

The aim of this project was to create a geological hazard assessment for managing the geological hazard, this model based on the Normalised Difference Vegetation Index with input raster data and DSRNN optimized with Whale Optimization Algorithm.

The main contribution of this research work is summarized as follows,

- In this research work, An Assessment of Geological Hazard Management using Dynamically Stabilized Recurrent Neural Network and Beluga Whale Optimization Algorithm (AGL-HM-DSRNN-BWOA) is proposed.
- In pre-processing the raster data are noise reduction and improving the quality using Adaptive Actor-Critic Bilateral Filter (A2CBF).
- Dynamically Stabilized Recurrent Neural Networks (DSRNN) is currently regarded as the most influential methods for classifying the efficacy of geological hazards.
- The obtained outcomes of proposed AGL-HM-DSRNN-BWOA algorithm is comparing to the existing models such as RA-IFA-GH-TME [20], LCC-NDVI-LRA [21], and MH-EM-SSA-ML [22] methods respectively.

Remaining manuscript is structured as: unit 2 outlines the Literature Survey, unit 3 displays the proposed method, unit 4 presents the results with discussions, unit 5 concluding this manuscript.

II. LITERATURE SURVEY

The literature presents a number of research projects on deep learning-based geological hazard managing assessment; this section evaluated some of the most recent studies.

Lin et al. [20] have presented Risk assessment with their influencing factors exploration of geological hazards in typical mountain environs. To determine the spatial pattern along influencing risk factors, the information quantity mode together with geo detector were used to build an evaluation index scheme under eight indicators: elevation, slope, normalized variance vegetation index, lithology, landuse category, average annual rain, remoteness from rivers and faults. The findings revealed that the environmental hazard was generally higher in southeast and lower in northwest, with a substantial spatial agglomeration pattern. Fully disclosing the danger has crucial implications for the local government's development of tailored preventative efforts. The method attains higher accuracy and lower sensitivity.

Dahigamuwa, et al. [21] have presented land cover categorization depending on normalized variance vegetation index for landslide risk valuation. The land cover categorization algorithms using NDVI from satellite pictures and its potential utility in predicting landslides. The technique may be able to effectively assess how land cover affects landslide dangers using NDVI as a stand-alone indicator. Another advantage would be

the ability to use satellite imaging to quickly identify undesirable activities, including deforestation. The categorization approach was used to a landslide-prone terrain in Oregon, USA. The results of five distinct classification methods—KNN, decision tree, ANN, Gaussian support vector machine (GSVM), and quadratic discriminant analysis—indicate that the NDVI-based land cover categorization was valid. The method attains higher sensitivity and lower specificity.

Nachappa et al. [22] have presented multiple hazard exposure mapping utilizing machine learning for Salzburg, Austria. A variety of exposure maps were created for thirteen flood and landslide influencing factors, including elevation, slope, aspect, topographic wetness with stream power indices, normalized variance vegetation index, geology, lithology, precipitation, land cover, distance from roads, drain. Divide the flood and landslide inventory data as training and validation using the commonly employed splitting ratio. The method attains higher specificity and lower accuracy.

Ahmad et al. [23] have presented four machine learning including statistical methods based geohazards susceptibility assessment with upper Indus basin. To produce susceptibility maps for geohazards including landslides and debris flows, Frequent Ratio (FR), Weights-of-Evidence (WoE), Logistic Regression (LR), and Stochastic Entropy (SE) were used. To achieve this, field data, historical hazard records, and remote sensing techniques were integrated to build a geohazard inventory. Investigations were conducted into the spatial relationship between hazard distribution and thirteen conditioning factors: slope, land cover, geology, elevation, the yearly average rainfall, the slope aspect, the remoteness from rivers, the profile curves, the stream power index, the topographic wetness index, the normalized variance plants index, and the land cover. The method attains higher ROC and lower sensitivity.

Zhang and Feng [24] have presented Multi sensor Information Fusion based Mine Geological Disaster Risk Assessment with Management. The multi sensor data integration was used for risk assessment of environmental hazards in mining. First describes the multisource data fusion process, which necessitates that the sensor first gather signals. It pre-processes the signals the sensor provides, and lastly examines the D-S evidence theory and BPNN fusion process in multi sensor data. A multisensor data integration technique were used to explore the deformers in the research region, evaluate their deformation and damage features, and assess the risk and susceptibility of the critical slopes. The method attains lower RMSE and higher MSE.

Prasetyo and Sembiring [25] have presented Tsunami Vulnerability and Risk Assessment in Banyuwangi District utilizing machine learning along Landsat eight image data. Machine learning was used to boost the vegetation index and intended to construct tsunami vulnerability assessment utilizing Vegetation Index collected from the Landsat eight satellite picture dataset and improved with KNN, RF,SVM. Although tsunamis were a frequent occurrence in Indonesia, there was no trustworthy indicator to assess and keep an eye on the coast based on the biophysical features of the earth surface or practical LULC. The vegetation index of LULC measures the severity of a tsunami's impact on a specific location. The method attains lower MSE and higher RMSE.

Dahim et al. [26] have presented Enhancing landslide management including hyper-tuned machine learning with deep learning approaches. To evaluate landslides in the Aqabat Al-Sulbat Asir region of Saudi Arabia using finely calibrated machine learning and deep learning algorithms, and to provide sensitivity and uncertainty assessments. Floods and landslides have had a major effect on people's lives, property, and natural resources. The growing human footprints in weak geological areas have resulted in an increase in the frequency of landslides, rendering landslide control a vital endeavour to mitigate the detrimental impact. The machine learning model was Random Forest (RF), while the deep learning model was Deep Neural Network (DNN). The grid-based search technique was utilized to optimize the hyper tuned models, which were then used to forecast LSM. This method attains lower mean absolute error and lower sensitivity.

III. PROPOSED METHODOLOGY

In this sector, an assessment of Geological Hazard Management using Dynamically Stabilized Recurrent Neural Network and Beluga Whale Optimization Algorithm (AGL-HM-DSRNN-BWOA) deliberated. Block diagram of proposed AGL-HM-DSRNN-BWOA method is in Figure 1. It covers such stages as Adaptive Actor-Critic Bilateral Filter, Dynamically Stabilized Recurrent Neural Network, and Beluga Whale Optimization Algorithm. Thus, detailed explanation about every steps given below,

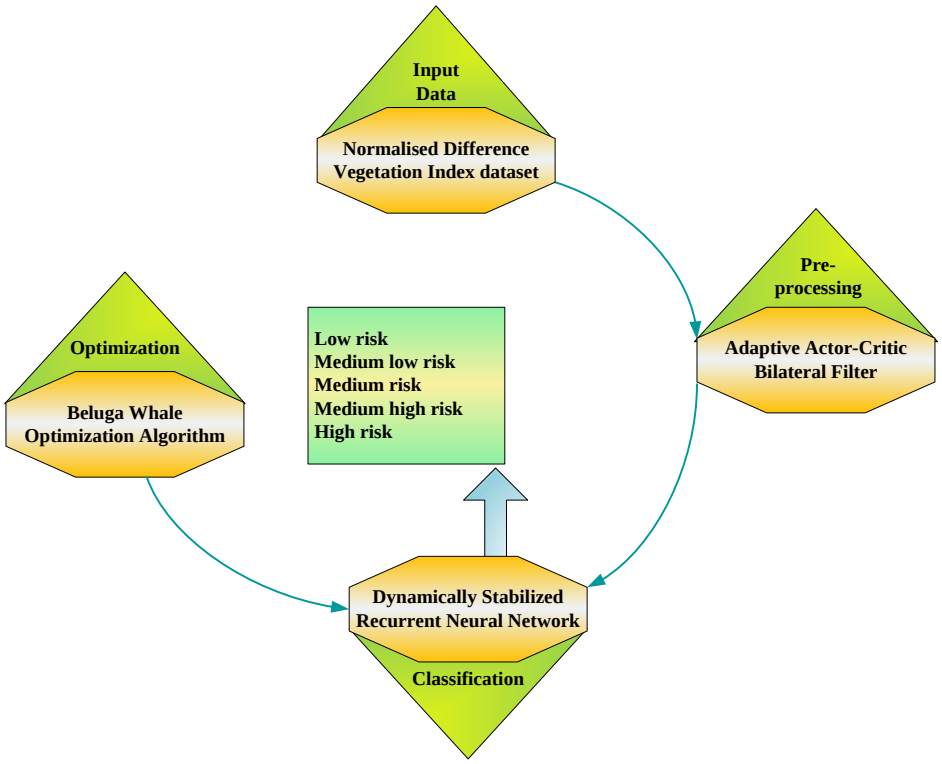

Figure 1: Block Diagram of Proposed AGL-HM-DSRNN-BWOA Method

A. Data Acquisition

The input raster data is collected through Normalised Difference Vegetation Index (NDVI) dataset [27]. This information are used for generating multi-source spatial data, which may then be united in the projected the WGS1984 coordinate scheme and packaged into a single 30m quality raster data.

B. Pre-Processing using Adaptive Actor-Critic Bilateral Filter

The pre-processing using Adaptive Actor-Critic Bilateral Filter (A2CBF) [28] is discussed here. The input raster data is pre-processed using A2CBF to remove noise and improving the quality of raster data. Adaptive approaches, such as adaptive actor-critic algorithms, have the ability to continuously modify their settings in response to changing geological conditions. This adaptability is essential for dealing with the dynamic and changing character of geological threats. The fundamental purpose of adopting adaptive actor-critic approaches and bilateral filters in geological hazard management is to increase risk assessment accuracy. This entails more accurately anticipating the likelihood and severity of geological events. This is due to the range kernel qualifies quantities related to raster data values. These are shown in equation (1)

$$\pi_J^* = \arg_{\pi_j} \max \mathrm{E}_{\pi_j} \left(\sum_{g=0}^{z} \gamma^g e_j^g \right) \tag{1}$$

Here z and g refers total raster data and steps, γ^g specifies g^{-th} power of discount factor. Reward e_j^g on j^{-th} raster data between two consecutive states. When filtering input is corrupted with smaller perturbations that are commonly imperceptible it has been shown in equation (2)

$$e^{th} = (\hat{f}_j - f_j^g)^2 - (\hat{f}_j - f_j^{g+1})^2 \tag{2}$$

Where, f_j^g denoted as a state, $\hat{f}_j$ is a ground-truth smoothed raster data, the filtering input raster data and the factors has been shown in the equation (3)

$$f_j^{g+1} = s(f_j^g; \sigma_j^g) \tag{3}$$

Each step from state $f^{(0)}$ and explores towards f^z, where z is total number of steps, s implies ordinary BF, σ^g signifies z^{-th} adaptive width-setting scheme for kernel range. In this method, the raster data point has the high quality of the filter to raster data resizing which has given in the equation (4)

$$\sigma_j^{g+1} = \sigma_j^g + a_j^g \tag{4}$$

Where, a_j^g denotes an action for each raster data in pre-defined set. Here, Adaptive Actor-Critic Bilateral Filter (A2CBF) is removed noise and increased the quality of raster data and the pre-processed raster data are given to geological hazard assessment process.

C. Geological Hazard Assessment using Dynamically Stabilized Recurrent Neural Network

This section describes the geological hazard assessment using DSRNN [29]. DSRNN is proposed to managing the geological hazard by assessment and it classifies as low risk, medium-low risk, medium-high risk, high risk. Dynamically Stabilized Recurrent Neural Networks are built to deal with consecutive data and temporal constraints. DSRNN would more likely improve the model's capacity to detect and learn complicated temporal trends in geological data, which is critical for hazard management. The main aim is anticipated to be more precise forecasting of geological dangers. This entails predicting when and where geological events will occur based on previous data and observable patterns. Skip-coefficients are configured as learnable parameters so that the DSRNN architecture can be stabilized by the network to measure the hidden state in equation (5)

$$g_t = \sum_{i=1}^{k} \{\alpha_i g_{t-i}\} + \varphi_g(g_{t-1}, w_t) \tag{5}$$

Where, g_t is a hidden state of the network, k denotes as a parameter, α_i is a diagonal matrix, $(\varphi_g(.))$ is an activation function and w_t is the input. For updating the skip coefficients and ensure the RNN states never diverge, regularize is applied to the loss function. This is continuously differentiable to the equilibrium point, which may be easily deemed to have the same origin. With the help of mean value theorem, the line connecting equilibrium point is given in equation (6)

$$p_{t+1} = \nabla_p e(p_t, w_t)\Big|_{\substack{pt=p^f \\ w_t=w^f}} p_t + \nabla_w e(p_t.w_t)\Big|_{\substack{p_t=p^f \\ w_t=w^f}} w_t + h.o.t. \tag{6}$$

Where, p_t denotes as state, p^f is the equilibrium pair, $e(.)$ is the neighbourhood of the equilibrium pair and $h.o.t$ implies high order for true nonlinear scheme. In particular, given a normal RNN without any skip connections, BPTT is established. This can be expressed in equation (7),

$$\frac{\partial \varepsilon_t}{\partial g_t - T} = \frac{\partial \varepsilon_t}{\partial g_t}\left(\sum_{i_1=1}^{k} \Delta g_{i_1}^0 \left(\sum_{i_2=1}^{k} \Delta g_{i_1+i_2}^{i_1}\right)\right) \tag{7}$$

Where, ε_t indicates error of RNN, T is the time-step. To demonstrate BPTT for the DSRNN for the situations, it gives two examples. Equation (8) reveals recurrent weight matrix's reatest singular value to show how the BPTT affects the gradient.

$$\frac{\partial \varepsilon_t}{\partial g_{t-0}} = \frac{\partial \varepsilon_t}{\partial g_t}\left(\Delta g_1^0 + \Delta g_2^0\right) \tag{8}$$

The errors are tracked back via a few branches until they reach the tree's edge, which represents the specific partial derivatives. It has to approach this problematic as an endeavour to go back four time steps, one or two steps at a time. This is shown in equation (9)

$$T = \mathrm{i} \times 1 + \mathrm{j} \times 2\big|_{i,j \in N} \tag{9}$$

If $(T=6)$ has 6 = 6×1 = 3×1+1×3 = 3×2, or $(i, j) \in ((6, 0), (3, 1), (0, 3))$, return back to the tree graph to reach (g_{t-6}), every pair of (i, j), here DSRNN managing the geological hazard by assessment, the associated term is given in the equation (10)

$$\binom{i+j}{i}\left(\frac{\partial g_t}{\partial g_{t-1}}\right)^i \cdot \left(\frac{\partial g_t}{\partial g_{t-2}}\right) \tag{10}$$

Then $\left(\frac{\partial \varepsilon_t}{\partial g_{t-6}}\right)$ derivation for DSRNN of parameter $(k=2)$, here the DSRNN has verified and extracted the bank cheque information automatically**,** and converted legal amount information using the proposed algorithm. Finally proposed DSRNN is managed the geological hazard by assessment and classified as low risk, medium low risk, medium high risk, high risk. In this work, BWOA is employed to optimize the DSRNN optimum parameters g_t *and* T. Here BWOA is employed for turning the weight and bias parameter of DSRNN.

D. Optimization using Beluga Whale Optimization Algorithm

In this section, Optimization using Beluga Whale Optimization Algorithm [30] is discussed. Here the DSRNNs weight parameters g_t *and* T are optimized using BWOA.BWOA, a nature-inspired optimisation technique, is intended for worldwide optimization. This means it has the capacity to exhaustively explore the solution space, which is useful for models using deep learning in geological hazard management while looking for optimal or near-optimal setups. The major purpose of applying the BWOA in deep learning for geological hazard management is most likely to identify optimal or near-optimal configurations for the models created using DSRNN. This entails optimizing hyper parameters and infrastructure to improve model performance. Especially, the absence of a transfer parameter during the transition from exploration to exploitation phase directly influences the performance of the algorithm. The initiation of BWOA involves the initialization step.

1) Stepwise processing of BWOA

The stepwise processing is delimited to acquire better value of NEGCN using BWOA. Initially, BWOA makes equal distributing populace to enhance the parameters g_t *and* T of NEGCN. Ideal solution promoted using BWOA algorithm.

Step 1: Initialization

The beluga whales are initially lured to the ocean current because it is rich in nutrients. The initial population is displayed in equation (11)

$$K=\begin{bmatrix} k_{1,1} & \cdots & k_{1,q} \\ \cdots & \cdots & \cdots \\ k_{1,a} & \cdots & k_{a,q} \end{bmatrix} \tag{11}$$

Generate the positions of the search agents in matrix K is denoted as Size; where a the population is size of the search agents, q implicates design variables.

Step 2: Random generation

Generate the input parameters randomly afterward the initialization. The ideal fitness value selection is depending upon their explicit hyperparameter situation.

Step 3: Fitness Function

The outcome is determined by initialization and random responses. The fitness is computed using the equation (12)

$$Fitness\,Function = Optimizing\ [g_t\ and\ T] \tag{12}$$

Step 4: Exploration Phase

This is inspired by the swimming behaviour of beluga whales, which display social-sexual behaviours in different positions, two beluga whales swim as pair closely using two modes. Thus, the beluga whales' pair swimming affects the search agents' positions. In this, the positioning of the search agents is updating by equation (13),

$$\begin{Bmatrix} K_{j,i}^{G+1} = K_{j,c_i}^{G} + \left(K_{e,c1}^{G} - K_{j,c_i}^{G}\right)(1+e_1)\sin(2\pi r_2), i = even \\ K_{j,i}^{G+1} = K_{j,c_i}^{G} + \left(K_{e,c1}^{G} - K_{j,c_i}^{G}\right)(1+e_1)\cos(2\pi r_2), i = odd \end{Bmatrix} \tag{13}$$

Where, G is the current iteration, $K_{j,i}^{G+1}$ epitomizes new positioning of j^{-th} beluga whale on i^{-th} dimension, c_j is chosen from d-dimension randomly, wherein the current positioning of j^{-th} beluga whale on c_j dimension indicates K_{j,c_i}^{G} the current position of e^{-th} and j^{-th} beluga whale represented as $K_{e,c1}^{G}$ and K_{j,c_i}^{G} respectively .Where E random beluga whale $(r_1,\ r_2)$ is randomly chosen (0, 1) to upgrade the

random operators $\sin(2\pi r_2)$ and $\cos(2\pi r_2)$. Figure 2 shows the flowchart for Beluga Whale Optimizing DSRNN.

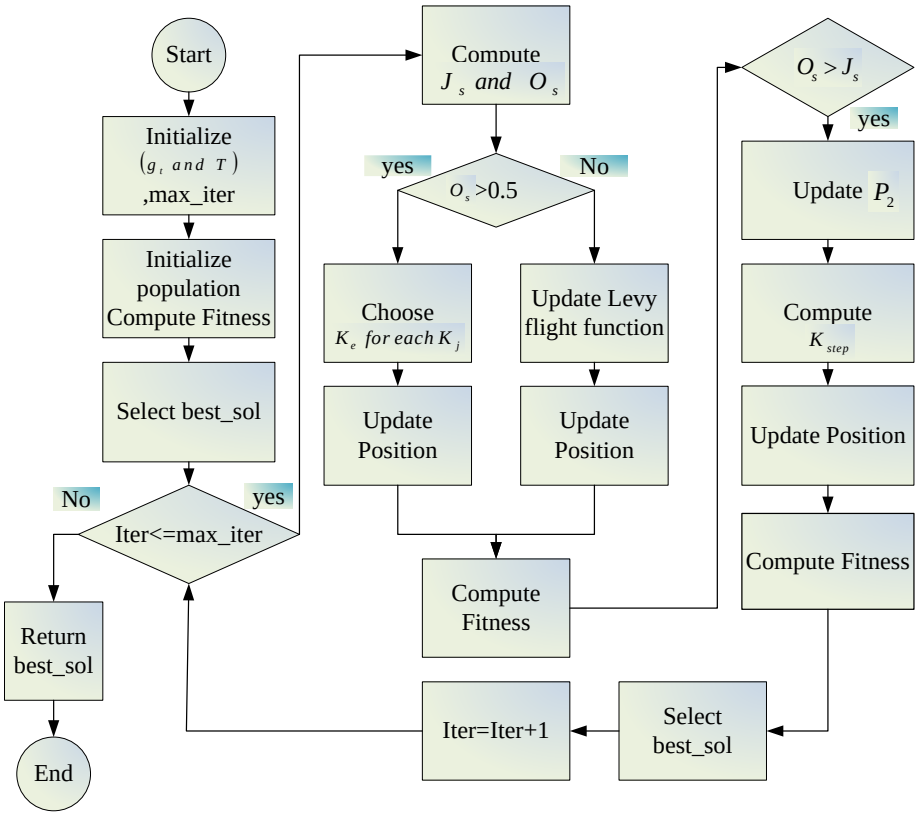

Figure 2: Flowchart for Beluga Whale Optimizing DSRNN

Step 5: Exploitation phase for optimizing g_t *and* T

Exploitation is the final stage; the goal of exploitation is to identify the best options within the promising areas. BWOAs exploitation phase is expressed in Equation (14)

$$L_J^{t(k)+1} = e_3 L_{best}^{t(k)} - e_4 L_j^{t(k)} + P_1.Y_S.(L_e^{t(k)} - L_j^{t(k)}) \tag{14}$$

The current iteration denotes G, a random beluga whale as well as current positioning of j^{-th} beluga whale implies $L_e^{t(k)}$, whereas $L_j^{t(k)}$ implies new positioning of j^{-th} beluga whale. The whole beluga whales are represented as $L_J^{t(k)+1}$ and K_{best}^G respectively, r_3 *and* r_4 are random numbers.

Step 6: Termination

The weight parameter g_t *and* T of generator from DSRNN is optimized under BWOA will repeat step 3 iteratively until fulfil the halting criteria $Iter = Iter + 1$. Finally, DSRNN has managed the geological hazard by assessment with higher accuracy.

IV. RESULT AND DISCUSSION

The experimental outcomes of the AGL-HM-DSRNN-BWOA technique are conferred in this sector. The proposed AGL-HM-DSRNN-BWOA method is implemented in Python platform with 12 GBRAM, Intel ®core (7M) i3-6100CPU @ 3.70GHz processor under performance metrics. The raster data are found using the NDVI dataset, NDVI values were calculated for each site location. NDVI was calculated by atmospherically adjusted Landsat TM data with spatial resolution of 30m x 30m. Data points are chosen stochastically 1km x 1km grid respectively. Bigger data sets typically take more time for training a model. The amount of sampling raster data or locations in collection with related NDVI values is an important consideration. Furthermore, the system's effectiveness is confirmed by contrasting the performance indicators of the proposed AGL-HM-DSRNN-BWOA approach with those of the existing methods, like RA-IFA-GH-TME, LCC-NDVI-LRA, and MH-EM-SSA-ML respectively.

A. Performance measures

This is a crucial step for determining the exploration of optimization algorithm. Performance measures to evaluate to access performance such as accuracy, sensitivity, specificity, ROC, MSE, RMSE, MAE.

1) Accuracy

Accuracy refers to the ability to measure a precise value. A statistic known as accuracy can be used to assess the performance across all classes. This is quantified by the following equation (15)

$$Accuracy = \frac{\left(TP + TN\right)}{\left(TP + FP + TN + FN\right)} \tag{15}$$

Here TP specifies True Positive, TN signifies True Negative, FP implies False Positive, FN implies False Negative.

2) Sensitivity

It measures the performance of a machine learning model to identify positive instances. In other words, it measures how likely it will get a positive result. This is calculated by equation (16)

$$Sensitivity = \frac{TP}{\left(TP + FN\right)} \tag{16}$$

3) Specificity

The fraction of True Negative accurately detected by the model is measured as specificity. This is also called as True Negative Rate. This is given in equation (17)

$$\text{Specificity} = \frac{TN}{\left(FP + TN\right)} \tag{17}$$

4) ROC

ROC curve portrays the true positive rate or sensitivity Vs false positive rate or 1-specificity. It is given in equation (18),

$$ROC = 0.5 \times \left(\frac{TP}{TP + FN} + \frac{TN}{TN + FP} \right) \tag{18}$$

5) Mean Square Error

This is calculated by averaging, or taking the mean, of all squared errors determined from data in relation to a function. The mean square error is given in equation (19),

$$Mean\,Square\,Error = \frac{1}{n} \sum_{i=1}^{n} (Y_i - \hat{Y}_i)^2 \tag{19}$$

6) Root mean square error

This is a two basic performance measures for a regression mode. It calculates the average variation among predicted values and actual values. This is given in equation (20),

$$\text{Root Mean Square Error} = \sqrt{\frac{1}{n} \sum_{i=1}^{n} (y_i - \hat{y}_i)^2} \tag{20}$$

7) Mean absolute error

This is often used in deep learning and regression applications to assess the accuracy of an algorithm's predictions. It calculates the average total disparity amongst the expected and actual values. The formula for Mean Absolute Error is as follows equation (21)

$$Mean\,Absolute\,Error = \frac{\sum_{i=1}^{n} | y_i - x_i |}{n} \tag{21}$$

B. Performance Analysis

The simulation results of AGL-HM-DSRNN-BWOA technique are shown in Figure 3 to 9. The proposed AGL-HM-DSRNN-BWOA techniques linked to the RA-IFA-GH-TME, LCC-NDVI-LRA, and MH-EM-SSA-ML techniques,

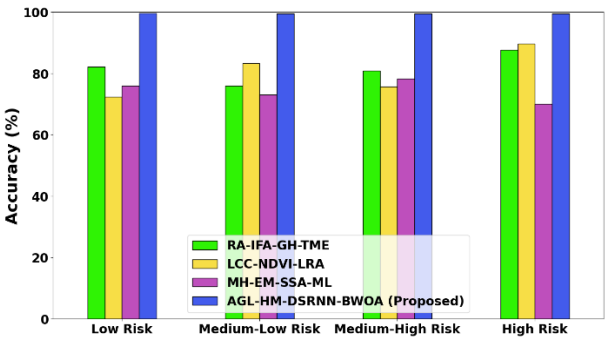

Figure 3: Accuracy analysis

Figure 3 shows Accuracy analysis. The AGL-HM-DSRNN-BWOA technique reaches in the range of 20.26%, 29.22% and 30.27% higher accuracy for low risk 27.29%, 18.31% and 16.26% higher accuracy for medium low risk 26.26%, 17.59% and 28.35% higher accuracy for medium high risk 29.21%, 26.38% and 25.25% higher accuracy for high risk compared to current techniques such as RA-IFA-GH-TME, LCC-NDVI-LRA, and MH-EM-SSA-ML respectively.

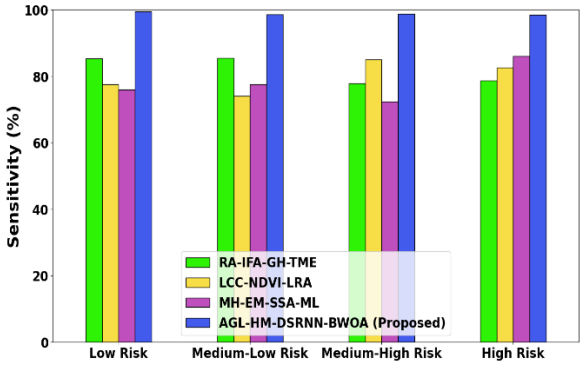

Figure 4: Sensitivity analysis

Figure 4 shows Sensitivity analysis. AGL-HM-DSRNN-BWOA technique reaches in the range of 21.26%, 19.22% and 28.27% higher sensitivity for low risk 19.29%, 25.31% and 25.26% higher sensitivity for medium low risk 27.26%, 29.59% and 19.35% higher sensitivity for medium high risk 24.21%, 19.38% and 23.25% higher sensitivity for high risk compared to current techniques such as RA-IFA-GH-TME, LCC-NDVI-LRA, and MH-EM-SSA-ML respectively.

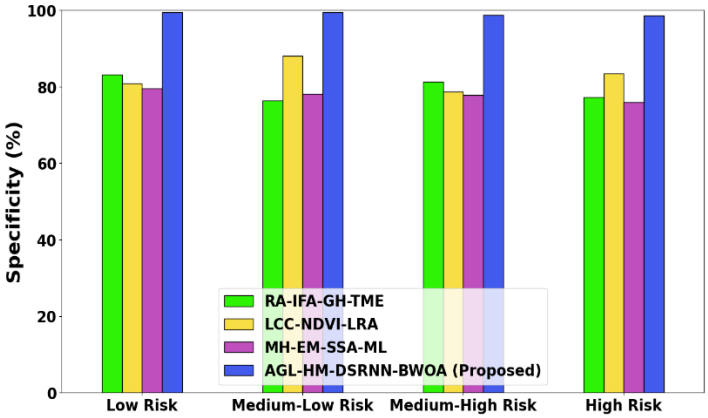

Figure 5: Specificity analysis

Figure 5 shows Specificity analysis. The AGL-HM-DSRNN-BWOA technique reaches in the range of 28.26%, 18.22% and 27.27% higher specificity for low risk 18.28%, 25.31% and 24.26% higher specificity for medium low risk 29.26%, 16.29% and 15.35% higher specificity for medium high risk 27.21%, 28.38% and 22.25% higher specificity for high risk compared to current techniques such as RA-IFA-GH-TME, LCC-NDVI-LRA, and MH-EM-SSA-ML respectively.

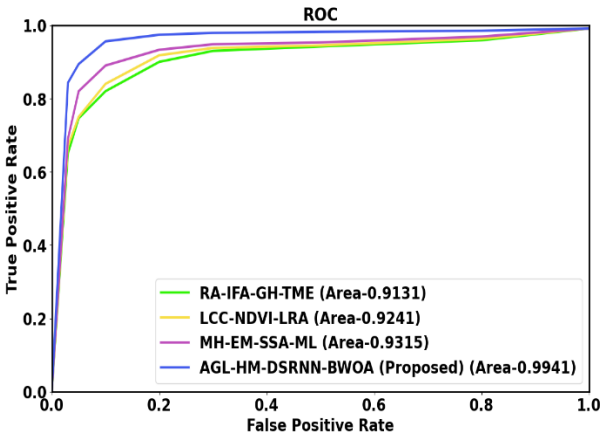

Figure 6: ROC analysis

Figure 6 shows ROC analysis. The AGL-HM-DSRNN-BWOA technique reaches in the range of 21.26%, 29.22% and 29.27% higher ROC compared to current techniques such as RA-IFA-GH-TME, LCC-NDVI-LRA, and MH-EM-SSA-ML respectively.

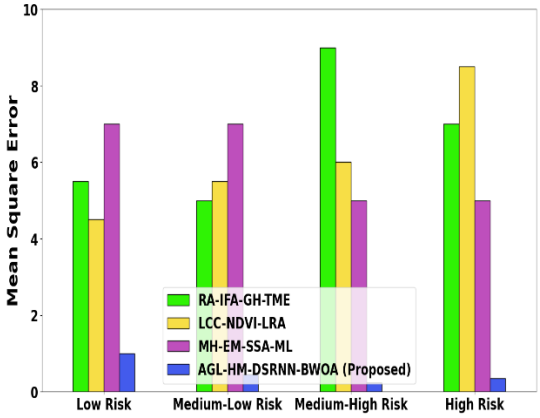

Figure 7: Mean Square Error analysis

Figure 7 shows MSE analysis. The AGL-HM-DSRNN-BWOA technique reaches in the range of 26.26%, 17.22% and 25.27% lower mean square error for low risk 29.29%, 24.31% and 21.26% lower mean square error for medium low risk 22.26%, 15.59% and 19.35% lower mean square error for medium high risk 26.21%, 28.38% and 29.28% lower mean square error for high risk compared to current techniques such as RA-IFA-GH-TME, LCC-NDVI-LRA, and MH-EM-SSA-ML respectively.

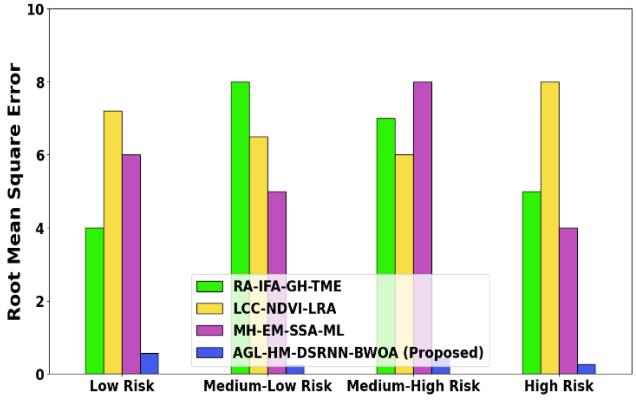

Figure 8: Root Mean Square Error analysis

Figure 8 shows RMSE analysis. The AGL-HM-DSRNN-BWOA technique reaches in the range of 28.26%, 15.22% and 22.27% lower root mean square error for low risk 29.29%, 24.31% and 27.26% lower root mean square error for medium low risk 27.26%, 17.59% and 28.35% lower root mean square error for medium high

risk 20.21%, 29.38% and 21.25% lower root mean square error for high risk compared to current techniques such as RA-IFA-GH-TME, LCC-NDVI-LRA, and MH-EM-SSA-ML respectively.

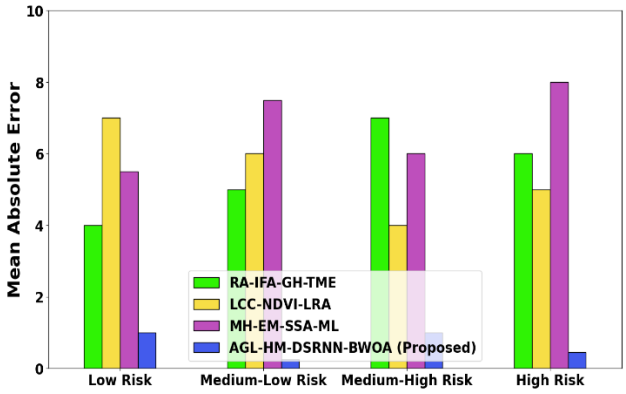

Figure 9: Mean Absolute Error analysis

Figure 9 shows MAE analysis. The AGL-HM-DSRNN-BWOA technique reaches in the range of 23.26%, 19.22% and 20.27% lower mean absolute error for low risk 19.29%, 28.31% and 26.26% lower mean absolute error for medium low risk 27.26%, 19.59% and 18.35%lower mean absolute error for medium high risk 19.21%, 29.38% and 28.25% lower mean absolute error for high risk compared to current techniques such as RA-IFA-GH-TME, LCC-NDVI-LRA, and MH-EM-SSA-ML respectively.

C. Discussion

This investigation utilized a model integrating eight factors to assess environmental hazard risks in Gansu Province, employing the information quantity model alongside geodetector analysis to characterize overall trends. Results indicate that geological hazards in Gansu are primarily of medium to medium-high risk, with fewer instances of high and low-risk events. Risk levels tend to be higher in the southeast and lower in the northwest, exhibiting distinct spatial patterns and agglomeration tendencies. High as well as medium-high risk zones are prevalent along the southeast coast, when lower risk regions are predominantly located at the northwest interior. These regional hazards result from a combination of natural and human factors, including night light intensity, elevation, distance from rivers, slope, lithology, annual rainfall, proximity to rivers, with the latter three factors exerting significant influence. The information quantity mode demonstrates higher reliability in risk assessment, as evidenced by spatial correspondence between hazard spots and risk levels, along with favourable ROC curve outcomes. It is imperative for local governments to formulate targeted strategies for mitigating geological catastrophes. This study has devised a framework for assessing the danger posed by geological hazards in Gansu Province, shedding light on spatial patterns and key risk factors. Such findings could enrich the government's disaster prevention plans, leveraging the region's unique terrain and geomorphology to enhance their scientific effectiveness.

V. CONCLUSION

In this paper**,** An Assessment of Geological Hazard Management using Dynamically Stabilized Recurrent Neural Network and Beluga Whale Optimization Algorithm (AGL-HM-DSRNN-BWOA) was successfully implemented. Here, NDVI dataset were used to assess the proposed technique. The proposed AGL-HM-DSRNN-BWOA method is executed in Python. The presentation of proposed AGL-HM-DSRNN-BWOA method covers 22.36%, 25.42% and 18.27% higher accuracy, 23.26%, 28.32% and 31.17% higher sensitivity, and 26.16%, 18.17% and 17.18% higher specificity compared with existing RA-IFA-GH-TME, LCC-NDVI-LRA, and MH-EM-SSA-ML methods. In the future process the proposed AGL-HM-DSRNN-BWOA model to maintain geological stability, urban construction should prioritize ecological conservation as a guiding concept. To ensure rapid growth in the economy, it's important to balance growth and security efforts. Land development prioritizes avoiding ecologically vulnerable and geologically hazardous places.

REFERENCE

[1] Ma, Z., & Mei, G. (2021). Deep learning for geological hazards analysis: Data, models, applications, and opportunities. *Earth-Science Reviews*, *223*, 103858.

[2] Bui, D.T., Tsangaratos, P., Nguyen, V.T., Van Liem, N., & Trinh, P.T. (2020). Comparing the prediction performance of a Deep Learning Neural Network model with conventional machine learning models in landslide susceptibility assessment. *Catena*, *188*, 104426.

[3] Liu, Y., & Wu, L. (2016). Geological disaster recognition on optical remote sensing images using deep learning. *Procedia Computer Science*, *91*, 566-575.

[4] Zhang, S., Tan, S., Geng, H., Li, R., Sun, Y., & Li, J. (2023). Evaluation of Geological Hazard Risk in Yiliang County, Yunnan Province, Using Combined Assignment Method. *Sustainability*, *15*(18), 13978.

[5] Wang, Z., Chen, Z., Ma, K., & Zhang, Z. (2023). Machine-Learning-Based Hybrid Modeling for Geological Hazard Susceptibility Assessment in Wudou District, Bailong River Basin, China. *GeoHazards*, *4*(2), 157-182.

[6] Isleyen, E., Duzgun, S., & Carter, R.M. (2021). Interpretable deep learning for roof fall hazard detection in underground mines. *Journal of Rock Mechanics and Geotechnical Engineering*, *13*(6), 1246-1255.

[7] Lu, Z., Yang, H., Zeng, W., Liu, P., & Wang, Y. (2023). Geological Hazard Identification and Susceptibility Assessment Based on MT-InSAR. *Remote Sensing*, *15*(22), 5316.

[8] Pourghasemi, H.R., Gayen, A., Edalat, M., Zarafshar, M., & Tiefenbacher, J.P. (2020). Is multi-hazard mapping effective in assessing natural hazards and integrated watershed management?. *Geoscience Frontiers*, *11*(4), 1203-1217.

[9] Yuan, R., & Chen, J. (2023). A novel method based on deep learning model for national-scale landslide hazard assessment. *Landslides*, *20*(11), 2379-2403.

[10] Fanos, A.M., Pradhan, B., Alamri, A., & Lee, C.W. (2020). Machine learning-based and 3d kinematic models for rockfall hazard assessment using LiDAR data and GIS. *Remote Sensing*, *12*(11), 1755.

[11] Yao, J., Qin, S., Qiao, S., Che, W., Chen, Y., Su, G., & Miao, Q. (2020). Assessment of landslide susceptibility combining deep learning with semi-supervised learning in Jiaohe County, Jilin Province, China. *Applied Sciences*, *10*(16), 5640.

[12] Tan, Q., Huang, Y., Hu, J., Zhou, P., & Hu, J. (2021). Application of artificial neural network model based on GIS in geological hazard zoning. *Neural Computing and Applications*, *33*, 591-602.

[13] Nikoobakht, S., Azarafza, M., Akgün, H., & Derakhshani, R. (2022). Landslide susceptibility assessment by using convolutional neural network. *Applied Sciences*, *12*(12), 5992.

[14] Youssef, A.M., Mahdi, A.M., & Pourghasemi, H.R. (2022). Landslides and flood multi-hazard assessment using machine learning techniques. *Bulletin of Engineering Geology and the Environment*, *81*(9), 370.

[15] Yin, D., Zhang, B., Yan, J., Luo, Y., Zhou, T., & Qin, J. (2023). CoWNet: A correlation weighted network for geological hazard detection. *Knowledge-Based Systems*, 110684.

[16] Wang, J., Sun, P., Chen, L., Yang, J., Liu, Z., & Lian, H., (2023). Recent Advances of Deep Learning in Geological Hazard Forecasting. *CMES-Computer Modeling in Engineering & Sciences*.

[17] He, F., Liu, H., Liu, C., & Bao, G. (2021). Analysis of radar technology identification model for potential geologic hazard based on convolutional neural network and Harris Hawks optimization algorithm. *Soft Computing*, 1-15.

[18] Khosravi, K., Panahi, M., Golkarian, A., Keesstra, S.D., Saco, P.M., Bui, D.T., & Lee, S. (2020). Convolutional neural network approach for spatial prediction of flood hazard at national scale of Iran. *Journal of Hydrology*, *591*, 125552.

[19] Wang, Z., Chen, J., Lian, Z., Li, F., Pang, L., & Xin, Y. (2024). Influence of buffer distance on environmental geological hazard susceptibility assessment. *Environmental Science and Pollution Research*, 1-14.

[20] Lin, J., Chen, W., Qi, X., & Hou, H. (2021). Risk assessment and its influencing factors analysis of geological hazards in typical mountain environment. *Journal of Cleaner Production*, *309*, 127077.

[21] Dahigamuwa, T., Yu, Q., & Gunaratne, M. (2016). Feasibility study of land cover classification based on normalized difference vegetation index for landslide risk assessment. *Geosciences*, *6*(4), 45.

[22] Nachappa, T.G., Ghorbanzadeh, O., Gholamnia, K., & Blaschke, T. (2020). Multi-hazard exposure mapping using machine learning for the State of Salzburg, Austria. *Remote Sensing*, *12*(17), 2757.

[23] Ahmad, H., Ningsheng, C., Rahman, M., Islam, M.M., Pourghasemi, H.R., Hussain, S.F., Habumugisha, J.M., Liu, E., Zheng, H., Ni, H., & Dewan, A. (2021). Geohazards susceptibility assessment along the upper Indus basin using four machine learning and statistical models. *ISPRS International Journal of Geo-Information*, *10*(5), 315.

[24] Zhang, D., & Feng, D. (2022). Mine Geological Disaster Risk Assessment and Management Based on Multisensor Information Fusion. *Mobile Information Systems*, *2022*.

[25] Prasetyo, S.Y.J., & Sembiring, I. (2023). Tsunami Vulnerability and Risk Assessment in Banyuwangi District using machine learning and Landsat 8 image data. *MATRIK: JurnalManajemen, TeknikInformatikadanRekayasaKomputer*, *22*(2), 365-380.

[26] Dahim, M., Alqadhi, S., & Mallick, J. (2023). Enhancing landslide management with hyper-tuned machine learning and deep learning models: Assessing susceptibility and analyzing sensitivity and uncertainty. *Frontiers in Ecology and Evolution*, *11*, 1108924.

[27] https://data.gov.au/dataset/ds-bom-ANZCW0503900404/details?q

[28] Chen, B.H., Cheng, H.Y., & Yin, J.L. (2022, May). Adaptive Actor-Critic Bilateral Filter. In *ICASSP 2022-2022 IEEE International Conference on Acoustics, Speech and Signal Processing (ICASSP)* (pp. 1675-1679). IEEE.

[29] Saab Jr, S., Fu, Y., Ray, A., & Hauser, M. (2022). A dynamically stabilized recurrent neural network. *Neural Processing Letters*, *54*(2), 1195-1209.

[30] Zhong, C., Li, G., & Meng, Z. (2022). Beluga whale optimization: A novel nature-inspired metaheuristic algorithm. *Knowledge-Based Systems*, *251*, 109215.